



Hydrogen transport parameters for a cobalt based alloy

Mickey R. Shanabarger

University of California, Santa Barbara, Santa Barbara, CA, 93106, USA

Abstract

Employing a basic, gas phase-permeation measurement procedure and modern, ultra-high vacuum technology, measurements were made of the hydrogen permeability and diffusivity in a commercially available Co based superalloy. The transport parameters were determined over a pressure range of $0.013\text{--}1.2 \times 10^5$ Pa and temperature range, 490–1150 K. The hydrogen solubility was estimated from the relationship between the permeability and diffusivity. The solubility obtained from these measurements is compared with published data for the equilibrium hydrogen solubility in pure Co. Similar anomalies are observed in both solubility measurements.

Keywords: Hydrogen; Solubility; Cobalt; Cobalt alloy

1. Introduction

The successful development of advanced aerospace propulsion systems based on hydrogen–oxygen fuels is dependent on the development of materials capable of successfully containing the high temperature, high pressure hydrogen. Studies have shown that cobalt based alloys appear to have higher resistance to mechanical property degradation in hydrogen environments compared with iron or nickel based alloys [1]. However, only recently were measurements initiated to determine the macroscopic transport parameters (permeability, diffusivity and solubility) for hydrogen in any Co based alloy system [2]. The alloy studied, Haynes 188 [3], is a commercially produced Co–Cr–Ni–W superalloy, whose measured composition is shown in Table 1. It is anticipated that the macroscopic transport parameters for this, as well as any alloy, may be influenced by the microstructure and chemical phases present in the alloy [4].

In the present report, a comparison is made between the hydrogen solubility in the cobalt alloy determined from the transport parameters and the equilibrium solubility in pure Co. The equilibrium solubility in Co was measured by Stafford and McLellan using the equilibrate–quench–vacuum extract method [5]. The solubility observed in their work has a non-Arrhenius temperature behavior which

they interpret as hydrogen trapping on grain boundaries. Hydrogen trapping is known to promote serious degradation of mechanical properties in iron and nickel based alloy systems [6].

Pure Co is known to undergo a structural phase transition from the low temperature hcp phase to a high temperature fcc phase at about 690 K [7]. The Haynes 188 alloy, which has an fcc crystal structure, is not reported to have any structural (or other) phase transformations [8]. It might be expected that the hydrogen solubility in the Co alloy would be comparable to the solubility observed at high temperature in pure Co, since they would both have the same crystal structure.

2. Experimental

In isothermal permeation studies involving metals, it is usually assumed that molecular hydrogen is dissociatively chemisorbed on the entrance side of a membrane of the material being studied. The chemisorbed hydrogen then diffuses through the bulk of the membrane as dissolved hydrogen. The dissolved hydrogen recombines on the exit side of the membrane to form molecular hydrogen which desorbs into the exit side volume where it is detected. For most experimental conditions, it is safe to assume that the surface processes (adsorption and desorption) occur rapidly compared to the time to diffuse through the membrane [9].

In the current study, the permeability, Φ , was obtained from measurements of the isothermal steady-state flux of hydrogen through the membrane, whereas the diffusivity, D , was obtained from a conventional lag-time analysis of

Table 1
Measured composition of Co alloy (Haynes 188) in atomic percent

Co	Cr	Ni	W	Fe	Other metallic	Non-metallic
44.0	24.6	23.1	4.6	1.7	0.9	1.2

the flux's transient response [10]. The solubility, S , is calculated using the measured permeability and diffusivity and the relationship, $S = \Phi/D$ [9]. The details of the hydrogen permeation apparatus and the general experimental procedures used in the present work are discussed elsewhere [2]. Only those elements important to the present discussion will be reviewed herein.

The permeation measurements were carried out in an ultra-high vacuum apparatus which could be baked out at high temperature to reduce impurity gases (the adsorption of which may affect the surface processes) and minimize the ever present hydrogen background, permitting permeation measurements at lower temperatures. The background pressure at the end of the bake-out period was typically $1\text{--}3 \times 10^{-6}$ Pa with the specimen at temperature. During the measurements, the exit side volume was continuously evacuated at a constant pumping speed so that the hydrogen partial pressure in the exit volume would be directly proportional to the flux of molecules permeating the membrane. The partial pressure in the exit volume was determined using a sensitive quadrupole mass analyzer. The permeation measurements were calibrated by comparing with independently calibrated leak sources traceable to NIST standards¹.

The Haynes 188 alloy permeation specimen was in the form of a closed-end cylinder, with the exterior surface of the cylinder being the exit side for the permeating hydrogen. The wall thickness of the cylinder in the gauge (membrane) section was 0.51×10^{-3} m (0.020 in.) with an interior radius of 4.76×10^{-3} m (3/16 in.). The gauge section was heated by an rf induction heater positioned over the gauge section. The temperature was measured with a thermocouple placed inside the specimen tube and contacting the interior wall in the center of the gauge section. The length of the isothermal region was 19.1×10^{-3} m (0.75 in.). The surfaces of the gauge section were mechanically polished and cleaned, both chemically and by repeated high temperature vacuum processing. The procedures employed produced repeatable data on a consistent basis as evidenced by the reproducibility of individual datum acquired randomly with some temperatures revisited months after the initial datum was acquired. In all the measurements the specimen was first heated under vacuum (both surfaces) to about 1073 K and held at temperature for 2–3 min to thoroughly outgas the gauge region. The gauge section was then allowed to cool to a temperature about 50 K below the target measurement temperature. The time record of the membrane temperature, entrance

side pressure, and exit side hydrogen partial pressure were digitally recorded during each measurement. The data were analyzed using the appropriate equations for permeation through a cylindrical membrane geometry [11].

3. Results and discussion

The data were obtained over a broad temperature range of 490–1150 K and an entrance side hydrogen pressure (p) range of 1.3×10^3 Pa to about 1.2×10^5 Pa. Except at the lowest temperatures, where pressure variation measurements were not performed, the permeation flux was observed to be proportional to \sqrt{p} . This result is demonstrated for data taken at high and moderated temperatures in Fig. 1. At lower temperatures, the time and signal sensitivity necessary to acquire adequately data becomes prohibitive. About 610 K was the lowest temperature where permeation flux data at multiple pressures could be reasonably acquired. These data scale with \sqrt{p} as shown by the two permeability data points at $1/T \sim 1.7 \times 10^{-3} \text{ K}^{-1}$ in Fig. 2. The result shown in Fig. 1 indicates that the subsurface hydrogen concentration in the cobalt alloy obeys Sievert's Law for the indicated conditions of temperature and pressure. This correspondence was not established in the earlier work on the equilibrium solubility of hydrogen in Co where measurements were made only at a constant pressure of 1 atm (1.01×10^5 Pa) [5].

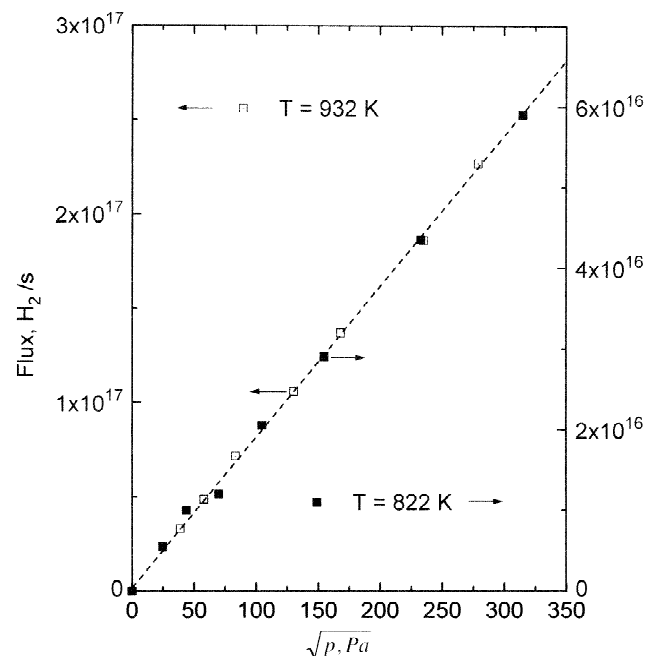


Fig. 1. The variation of the hydrogen flux permeating a Co alloy specimen (Haynes 188) as a function of the entrance side H_2 pressure, p , at two different temperatures, 822 K and 932 K.

¹The calibrated H_2 leaks were manufactured by Vacuum Instruments Corp., Ronkonkoma, NY and had values of 3.26×10^{-6} (at 23.3°C) and 7.85×10^{-5} (at 25.0°C) atm-cc s^{-1} .

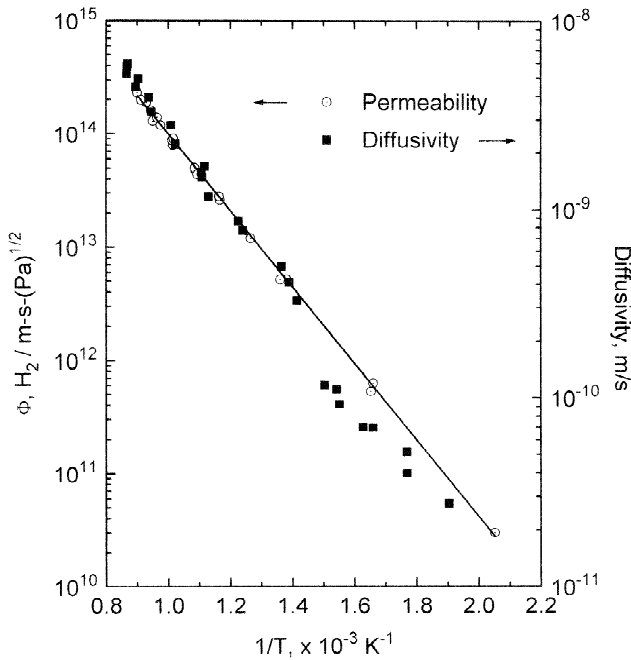


Fig. 2. The temperature dependence of the permeability, Φ , and diffusivity, D , of hydrogen in a Co alloy (Haynes 188).

3.1. Permeability and diffusivity

The temperature dependence of the permeability (Φ) is shown as an Arrhenius plot in Fig. 2. The permeability data is accurately described by a single activation energy Arrhenius relationship over the entire temperature range,

$$\Phi = 2.4 \times 10^{17} \exp(-64.6/RT), \text{H}_2/\text{m} - \text{s} - (\text{Pa})^{1/2} \quad (1)$$

The gas constant R is in units of $\text{kJ}/\text{mole} \cdot \text{K}$ and T is the temperature in Kelvin.

The diffusivity (D) was determined from an analysis of the “lag-time,” where the “lag-time” is the time axis intercept of the straight line, long time behavior of the time integral of the permeation flux [11]. The flux data was acquired for a time period exceeding 4–5 times the “lag-time” to insure adequate accuracy. The temperature dependence of the diffusivity is presented as an Arrhenius plot in Fig. 2. Unlike the permeability data, the diffusivity cannot be accurately fitted by a single activation energy Arrhenius relationship. The data indicates that the magnitude and temperature dependence of the diffusivity changes abruptly at about 690 K. Above and below the transition temperature, the diffusivity is represented by the following:

$$D = 4.6 \times 10^{-7} \exp(-42.3/RT), \text{m}^2/\text{s}, \text{ for } T > 690 \text{ K}$$

and

$$D = 2.0 \times 10^{-8} \exp(-28.4/RT), \text{m}^2/\text{s}, \text{ for } T < 690 \text{ K}.$$

3.2. Solubility

The hydrogen solubility was calculated using the thermodynamic relationship, $S = \Phi/D$. In determining S , the permeability and diffusivity data points were not always acquired at the same temperature, so the accurate fit to the permeability data, Eq. (1), was used to estimate the Φ value at each diffusivity datum temperature. The solubility values generated by this procedure are presented as an Arrhenius plot in Fig. 3. To be consistent with the equilibrium solubility data of Stafford and McLellan for Co [12], shown also in Fig. 3, the Co alloy solubility has been evaluated for one atmosphere hydrogen pressure ($1 \times 10^5 \text{ Pa}$).

As can be seen from Fig. 3, the hydrogen solubility in the Co alloy and Co are very similar in terms of their temperature dependence, magnitude and the presence of a high–low temperature transition. For the Co alloy, the solubility can be accurately fitted to the following:

$$S(1 \text{ atm}) = 1.47 \times 10^{26} \exp(-21.1/RT), \text{H}_2/\text{m}^3,$$

$$\text{for } T > 690 \text{ K}$$

and

$$S(1 \text{ atm}) = 21.1 \times 10^{26} \exp(-33.1/RT), \text{H}_2/\text{m}^3,$$

$$\text{for } T < 690 \text{ K}.$$

Stafford and McLellan concluded that the anomalous

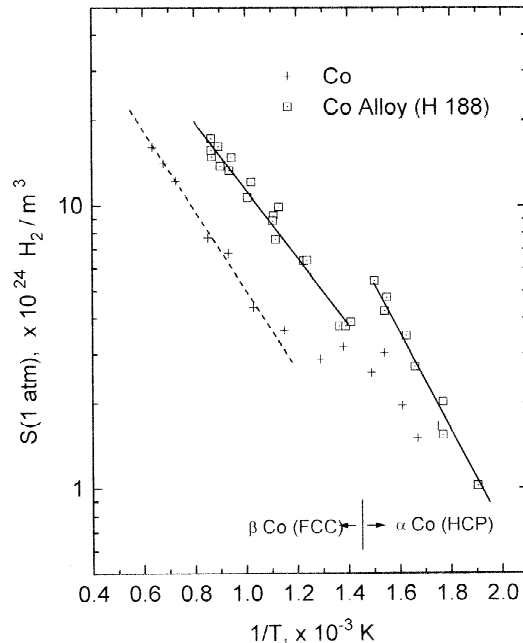


Fig. 3. The temperature dependence of the solubility, S , of hydrogen at one atmosphere ($1 \times 10^5 \text{ Pa}$) in a Co alloy (Haynes 188) and pure Co ([12]).

behavior observed in the equilibrium solubility for hydrogen in Co was due to the trapping of dissolved hydrogen, possibly at grain boundaries. Such transitions, however, are quite gradual and not as abrupt as implied by their data [6,11]. Crystallographic phase transitions, on the other hand, do show abrupt transitions similar to the cobalt data [13]. The solubility transition for Co, however, occurs at a temperature higher than the α - β transition temperature, see Fig. 3.

There are no reported bulk phase transitions for the Co alloy, nor is evidence of any transition present in measurements of various physical parameters [8]. It is possible, however, that a transition is occurring at the grain boundaries which act as a source of trapping sites. In the Ni-C system, for example, there is a sharp temperature transition for the segregation of C from the bulk to a free surface; below the transition temperature, C is present on the free surface with a fixed concentration and above the transition temperature, the C nearly completely dissolves in the bulk [14]. If the surface C was acting as a grain boundary hydrogen trap in Ni, then evidence of trapping would abruptly appear at temperatures below the transition temperature. The temperature dependence of the equilibrium solubility of hydrogen in polycrystalline Ni [5] does exhibit the same abrupt temperature transition as observed in Co and the Co alloy. The transition is absent in equilibrium solubility studies using Ni single crystals [5]. In single crystals, the absence of grain boundaries (except at the free surface) would be expected to significantly reduce the effectiveness of a surface transition-trapping mechanism.

If the solubility anomaly in the Co alloy is caused by trapping, then it can be inferred that the trapping process may be more activated than for the lattice diffusion process, i.e. the activation barrier between the dissolved state and the trapped state is larger than between adjacent dissolved states. The Co alloy data in Fig. 3 implies that as the temperature decreases, the solubility approaches values obtained by extrapolation from the high temperature data. This suggests that the traps are losing their effectiveness at lower temperatures. This is consistent with thermal activation being required to initially populate the traps. At the lower temperatures, the dissolved hydrogen does not have enough energy to cross the additional activation barrier and reach the trap. Confirmation of this hypothesis requires additional measurements at lower temperatures. Such measurements are in progress along with surface studies to investigate the possibility of a surface phase transition in the Co alloy.

4. Summary

The hydrogen permeability and diffusivity have been measured in a cobalt based alloy (Haynes 188) over a temperature range of 490–1150 K and a pressure range of

0.013– 1.2×10^5 Pa. The permeating hydrogen flux was found to be proportional to \sqrt{p} , where p is the entrance side hydrogen pressure indicating that the Co alloy obeys Sievert's Law.

The hydrogen permeability can be accurately fit over the entire temperature range to the following Arrhenius relationship: $\Phi = 2.4 \times 10^{17} \exp(-64.6/RT) \text{ H}_2/\text{m-s}(\text{Pa})^{1/2}$. Here R is in units of kJ/mole·K and T is the temperature in K. The temperature dependence of the diffusivity which was obtained from measurements of the "lag-time," shows a discontinuity and cannot be fit to a single activation energy. The high temperature component of the diffusivity should represent the lattice diffusivity of hydrogen in the Co alloy. It is postulated that the low temperature diffusivity results from an activated trapping process associated with a grain boundary carbon solubility phase transition. The lattice diffusivity for temperatures greater than 690 K is represented by the following; $D = 4.6 \times 10^{-7} \exp(-42.3/RT), \text{ m}^2 \text{ s}^{-1}$.

The solubility derived from the permeability and diffusivity is in reasonable agreement with the equilibrium solubility obtained elsewhere for Co, including the presence of a temperature dependent discontinuity. The high temperature component of the solubility should be representative of the lattice hydrogen solubility in the Co alloy and is represented by the following: $S = 4.6 \times 10^{23} \exp(-21.1/RT), \text{ H}_2/\text{m}^3(\text{Pa})^{1/2}$ for temperatures greater than 690 K.

Acknowledgments

This work was performed at NASA-Ames Research Center with financial support provided by a National Aeronautics and Space Administration Cooperative Agreement, NCC-2-63.

References

- [1] B.N. Bhat, R.L. Dreshfield and E.J. Veseley, Jr., (eds.), *Second Workshop on Hydrogen Effects on Materials in Propulsion Systems*, NASA Conference Publication 3182, 1992.
- [2] M.R. Shanabarger, Comparison of the High Temperature Hydrogen Transport Parameters for the Alloys Incoloy 909, Haynes 188, and Mo-47.5Re, in: A.W. Thompson and N.R. Moody, (eds.), *Hydrogen Effects in Materials*, The Minerals, Metals and Materials Society, Warrendale, PA, 1996, p. 243.
- [3] Haynes 188 is a trademark of Haynes International, Inc., Kokomo, Indiana.
- [4] For examples, see the discussions in N.R. Moody and A.W. Thompson, (eds.), *Hydrogen Effects on Material Behavior*, Section 1, The Minerals, Metals and Materials Society, Warrendale, PA, 1990, pp. 3–249.
- [5] S.W. Stafford and R.B. McLellan, *Acta Metal.*, 22 (1974) 1463.
- [6] H.H. Johnson, Hydrogen and Deuterium Trapping in Iron, in: I.M. Bernstein and A.W. Thompson, (eds.), *Hydrogen Effects in Metals*, The Metallurgical Society, Warrendale, PA, 1981, p. 3.
- [7] C.J. Smithells and E.A. Brandes, (eds.), *Metals Reference Book*,

- Buttersworth & Co., London, 1976; also in: T. Lyman, (ed.) *Metals Handbook*, American Society for Metals, Metals Park, OH, 1961, Vol. 1, p. 1202.
- [8] Haynes Alloy Product Information Sheet, H-3001A Haynes International, Inc, Kokomo, IN, 1991.
- [9] To uniquely establish that the transport process is dominated by bulk diffusion, it is necessary to show that the permeation flux is proportional to \sqrt{p} and that the lag-time is inversely proportional to the membrane thickness (see references cited in: D.K. Kuhn and M.R. Shanabarger, *Hydrogen Effects on Material Behavior*, p. 33). The work being reported herein is for a single membrane thickness.
- [10] R. Ash and R.M. Barrer, *Phil. Mag.*, 4 (1959) 1197.
- [11] H.G. Nelson and J.E. Stein, *Gas Phase Hydrogen Permeation through Alpha Iron, 4130 Steel, and 304 Stainless Steel From Less Than 100 ' to Near 600 C*, NASA Technical Note, NASA TN, D-7265, 1973.
- [12] The equilibrium solubility data for Co was taken from Table 1 of S.W. Stafford and R.B. McLellan, loc. cit.
- [13] See Figure 3 in S.W. Stafford and R.B. McLellan, loc. cit., where data on the temperature dependence of the solubility of hydrogen in Fe is presented. The temperature range encompasses the α - γ and γ - δ solid phase transitions.
- [14] J.C. Shelton, H.R. Patil and J.M. Blakely, *Surface Sci.*, 43 (1974) 493.